Universiteit Leiden
The Netherlands

Structure–activity relationship of 2,4-D correlates auxinic activity with the induction of somatic embryogenesis in Arabidopsis thaliana

Karami, O.; Jong, H. de; Somovilla, V.J.; Villanueava Acosta, B.; Sugiarta, A.B.; Ham, M.; ... ; Offringa, R.

Citation
Karami, O., Jong, H. de, Somovilla, V. J., Villanueava Acosta, B., Sugiarta, A. B., Ham, M., ... Offringa, R. (2023). Structure–activity relationship of 2,4-D correlates auxinic activity with the induction of somatic embryogenesis in Arabidopsis thaliana. *The Plant Journal*, *116*(5), 1355-1369. doi:10.1111/tpj.16430

Version: Publisher's Version
License: Creative Commons CC BY 4.0 license
Downloaded from: https://hdl.handle.net/1887/3716523

Note: To cite this publication please use the final published version (if applicable).

Check for updates

the plant journal

SEB SOCIETY FOR EXPERIMENTAL BIOLOGY

The Plant Journal (2023) **116,** 1355–1369 doi: 10.1111/tpj.16430

Structure–activity relationship of 2,4-D correlates auxinic activity with the induction of somatic embryogenesis in *Arabidopsis thaliana*

Omid Karami[1,†], Hanna de Jong[2,†], Victor J. Somovilla[3], Beatriz Villanueva Acosta[1], Aldo Bryan Sugiarta[1], Marvin Ham[1,‡], Azadeh Khadem[1,§], Tom Wennekes[2] and Remko Offringa[1,*]

[1]*Plant Developmental Genetics, Institute of Biology Leiden, Leiden University, Sylviusweg 72, 2333 BE Leiden, Netherlands,*
[2]*Department of Chemical Biology and Drug Discovery, Utrecht Institute for Pharmaceutical Sciences and Bijvoet Center for Biomedical Research, Utrecht University, Universiteitsweg 99, 3584CG Utrecht, The Netherlands,*
[3]*Center for Cooperative Research in Biomaterials (CIC biomaGUNE), Basque Research and Technology Alliance (BRTA), Paseo de Miramon 182, 20014 Donostia San Sebastián, Spain*

Received 5 July 2022; revised 19 July 2023; accepted 4 August 2023; published online 30 August 2023.
*For correspondence (e-mail r.offringa@biology.leidenuniv.nl).
[†]These authors contributed equally to this work.
[‡]Present address: Seed Genetics, Seed Technology Research, Rijk Zwaan, Burgemeester Crezeelaan 40 2678 KX, De Lier, The Netherlands
[§]Present address: Department of Horticultural Plants Biotechnology, Research Institute of Industrial Biotechnology, Academic Centre for Education, Culture and Research (ACECR), Khorasan Razavi Branch, Mashhad, Iran

SUMMARY

2,4-dichlorophenoxyacetic acid (2,4-D) is a synthetic analogue of the plant hormone auxin that is commonly used in many *in vitro* plant regeneration systems, such as somatic embryogenesis (SE). Its effectiveness in inducing SE, compared to the natural auxin indole-3-acetic acid (IAA), has been attributed to the stress triggered by this compound rather than its auxinic activity. However, this hypothesis has never been thoroughly tested. Here we used a library of forty 2,4-D analogues to test the structure–activity relationship with respect to the capacity to induce SE and auxinic activity in *Arabidopsis thaliana*. Four analogues induced SE as effectively as 2,4-D and 13 analogues induced SE but were less effective. Based on root growth inhibition and auxin response reporter expression, the 2,4-D analogues were classified into different groups, ranging from very active to not active auxin analogues. A halogen at the 4-position of the aromatic ring was important for auxinic activity, whereas a halogen at the 3-position resulted in reduced activity. Moreover, a small substitution at the carboxylate chain was tolerated, as was extending the carboxylate chain with an even number of carbons. The auxinic activity of most 2,4-D analogues was consistent with their simulated TIR1-Aux/IAA coreceptor binding characteristics. A strong correlation was observed between SE induction efficiency and auxinic activity, which is in line with our observation that 2,4-D-induced SE and stress both require TIR1/AFB auxin co-receptor function. Our data indicate that the stress-related effects triggered by 2,4-D and considered important for SE induction are downstream of auxin signalling.

Keywords: *Arabidopsis thaliana*, 2,4-dichlorophenoxyacetic acid (2,4-D), somatic embryogenesis, auxin analogue, auxinic activity, root system architecture.

INTRODUCTION

The plant hormone auxin plays a central role in the development of plants. In the 1930s, the structure of the natural auxin indole-3-acetic acid (IAA) was first described (Ma et al., 2018). Several years later, during WWII, 2,4-dichlorophenoxyacetic acid (2,4-D) was discovered as a synthetic auxin analogue that can be used as a herbicide, targeting dicots. Today, it is still broadly used as such in gardens and in agriculture (Peterson et al., 2016). Apart from the cell elongation-promoting effect, which led to its discovery as auxin analogue, 2,4-D acts differently in various physiological and molecular assays compared to the natural auxin IAA (Calderón Villalobos et al., 2012; Peterson et al., 2016; Shimizu-Mitao & Kakimoto, 2014).

Binding of IAA to its receptors triggers a transcriptional response. The classical nuclear IAA signalling pathway relies on the degradation of the transcriptional AUXIN/INDOLE-3-ACETIC ACID (Aux/IAA) repressors, leading to

© 2023 The Authors.
The Plant Journal published by Society for Experimental Biology and John Wiley & Sons Ltd.
This is an open access article under the terms of the Creative Commons Attribution License, which permits use, distribution and reproduction in any medium, provided the original work is properly cited.

the expression of auxin-responsive genes (Leyser, 2018). The degradation of Aux/IAAs is initiated by the binding of auxin to the F-Box proteins TRANSPORT INHIBITOR RESISTANT1 (TIR1) or AUXIN SIGNALING F-BOX 1–3 (AFB1-3). Auxin acts as a molecular glue, allowing the TIR1/AFBs to recruit the N-terminal domain II of Aux/IAAs (Winkler et al., 2017). TIR1/AFBs are part of an Skp1-Cullin-F-box (SCF) E3 ubiquitin ligase complex, which after recruiting Aux/IAAs marks these proteins for degradation by the 26S proteasome (dos Santos Maraschin et al., 2009; Iglesias et al., 2018).

The synthetic auxin 2,4-D elicits a dual response in plants, as it acts as an auxin and also induces stress (Karami & Saidi, 2010; Song, 2014). Like IAA, 2,4-D acts through the TIR1/AFB auxin-mediated signalling pathway (Calderón Villalobos et al., 2012; Shimizu-Mitao & Kakimoto, 2014; Song, 2014). At high concentrations, 2,4-D acts as herbicide and selectively kills dicot weeds. The herbicidal activity of 2,4-D can be attributed to several effects, including the altering of cell wall plasticity and the increase of ethylene levels (Song, 2014). The overproduction of ethylene triggers the increased production of abscisic acid (ABA), which contributes to stomatal closure and thus eventually to plant death (Karami & Saidi, 2010; Song, 2014). 2,4-D also induces the production of reactive oxygen species (ROS) that are very toxic to the plant (Karami & Saidi, 2010).

Besides its use as a herbicide, 2,4-D is widely used for biological experiments to induce auxin responses and for *in vitro* regeneration systems. Our interest in 2,4-D lies in its ability to efficiently induce somatic embryogenesis (SE) at non-herbicidal concentrations. SE is a unique developmental process in which differentiated somatic cells can acquire totipotency and are 'reprogrammed' to form new 'somatic' embryos. SE is a powerful tool in plant biotechnology used for clonal propagation, genetic transformation and somatic hybridization. It prevents somaclonal variation that is often observed in plant tissue culture, and somatic embryos can be easily cryopreserved (Guan et al., 2016; Horstman et al., 2017). Although SE can be induced by IAA, other synthetic auxins, or stress, in many cases 2,4-D is most effective and it is therefore widely used for SE in many plant species (Fehér, 2015; Karami & Saidi, 2010). Different observations have led to the suggestion that signalling pathways activated by abiotic stress treatments and 2,4-D treatment converge to trigger a common downstream pathway (Fehér, 2015). 2,4-D induced SE is accompanied by upregulation of stress-related genes (Jin et al., 2014; Nowak et al., 2015; Salvo et al., 2014), and several stress-related transcription factors have been shown to influence the progression of SE (Gliwicka et al., 2013; Mantiri et al., 2008; Nowak et al., 2015). This suggests that stress induced by non-herbicidal concentrations of 2,4-D (Fehér, 2015) contributes significantly to its effectiveness as an SE inducer. To further understand 2,4-D-induced SE, we established a structure–activity relationship (SAR) of 2,4-D with respect to its capacity to induce SE and activity as an auxin analogue.

Previous studies have already discovered several chemical analogues of 2,4-D with auxin-like activity. Unfortunately, however, several different bioassays have been used in these studies (Ferro et al., 2010), making a direct comparison difficult. In addition, several possible 2,4-D analogues that based on these previous studies would be interesting candidates to assess in a structure–activity relationship (SAR) have not been tested yet. Here, we, therefore, formed a rationally designed library of 40 2,4-D analogues and screened them for SE induction and auxinic activity in *Arabidopsis thaliana* (Arabidopsis). Four analogues induced SE as effectively as 2,4-D and 13 analogues did induce SE but were less effective. Based on root growth inhibition, root hair and lateral root induction, and auxin response reporter expression we classified compounds as very active, active, weakly active or inactive auxins, or even having anti-auxin activity. From the SAR, we concluded that a halogen at the 4-position of the aromatic ring is important for auxinic activity, whereas a halogen at the 3-position has a negative effect. Moreover, a small substitution at the carboxylate chain, a methyl or ethyl group, is tolerated, as is extending the carboxylate chain with two but not with one carbon. Molecular dynamics simulations indicated that the classification of the 2,4-D analogues reflected the binding characteristics (enthalpy and distance) to TIR1. SE induction capacity is clearly correlated with auxinic activity, indicating that the stress response induced by 2,4-D treatment and reported to be required for SE induction is downstream of auxin signalling.

RESULTS

Assembly of the 2,4-D analogue library

We aimed to screen a library of 2,4-D analogues for SE induction and auxinic activity in Arabidopsis and thereby gain insight into the SAR for this process. To this end, we first performed a literature survey of key past auxin studies in order to identify known 2,4-D analogues for our library (Ferro et al., 2007, 2010; Hayashi et al., 2012; Katekar, 1979; Koepfli et al., 1938; Lee et al., 2014; Quareshy et al., 2018; Song, 2014; Tan et al., 2007). This provided an overview of auxin activities and the binding efficiencies of some 2,4-D-like compounds to the auxin co-receptors and gave some context on the SAR of auxin-like compounds. In addition, it offered insight into the difficulties encountered in the past in establishing a SAR, such as non-standardized assays and the use of impure compounds. However, a rational SAR of 2,4-D could not be deduced from these past studies. To achieve a more complete SAR of 2,4-D with respect

© 2023 The Authors.

1365313x, 2023, 5, Downloaded from https://onlinelibrary.wiley.com/doi/10.1111/tpj.16430 by University Of Leiden, Wiley Online Library on [28/11/2023]. See the Terms and Conditions (https://onlinelibrary.wiley.com/terms-and-conditions) on Wiley Online Library for rules of use; OA articles are governed by the applicable Creative Commons License

to the induction of SE and auxinic activity, we assembled our own library with TIR1 as the target co-receptor, 2,4-D as a lead compound, analogue hits from the literature survey and several additional structures to achieve a more complete and rational coverage of possible 2,4-D analogues. In general, analogues of the lead compound 2,4-D, either commercially available or synthesized (Supplementary Data S1), were selected based on modifications at two positions: the type and number of substituents on the aromatic ring or on the alpha position of the carboxylate side chain (**F**igure 1a). A complete overview of the library is provided in Figure 1b.

Somatic embryogenesis induction by 2,4-D analogues

As a first step, we tested the ability of all 2,4-D analogues (Figure 1) to induce SE in Arabidopsis immature zygotic embryos (IZEs), which in prior studies has proven to be the most competent Arabidopsis tissue for SE in response to 2,4-D (Gaj, 2001).

In this assay, where each compound was tested at the same concentration as 2,4-D (5 μM), four compounds (class 1: 4-Cl, 4-Br, 2,4-DP, 2,4-Br) were able to efficiently induce somatic embryos from IZEs to a similar extent as 2,4-D (Figure 2a,b). Thirteen other compounds (class 2: 2,4-DB, 2-Cl-4-F, MCPA, Mecoprop, 4-F, 4-I, 2,5-D, 3,4-D, 2-F-4-Cl, 2-F-4-Br, 2,4,5-T, 2,4-DiB and MCPB) did induce somatic embryos on IZEs but were less effective compared with 2,4-D (Figure 2a,b). The remaining auxin analogues (class 3: 2-Cl, 2-I, 3-Cl, 2,6-D, 3,5-D, 2,4-F, 2,3,4-F, 2,3,4-T, 2-NO2-4-Cl, 2,4-DnB, PHAA, 4-NO_2, 3,5-Me, 2-Cl-4-formyl, and 2,4,6-F, 3-Me, 2,3-D, 3,5-D, 2,4,6-T and 2,4-DnP) did not induce SE (Figure S1). Overall, the capacity of compounds to induce SE seemed to correlate with their 2,4-D-like structure.

Generating a detailed dose–response curve for all compounds was beyond the scope of our research. However, to test whether the 5 μM concentration used was sufficient, we applied several class 1 and class 2 compounds at a 2-fold higher concentration. For 2,4-D, 4-Br, 4-I or MCPA this reduced the number of embryos formed on IZEs, whereas for 4-Cl, 4-F or 2,4,5-T this had no significant effect on the SE efficiency (Figure 2b). The results indicate that, like for 2,4-D, 5 μM is more or less optimal for the class 1 compounds, and that the lower SE efficiency obtained with the class 2 compounds cannot be compensated for by applying them at a higher concentration.

Assessing auxinic activity of the 2,4-D analogues based on root growth inhibition

Exogenous auxin inhibits primary root elongation in Arabidopsis in a concentration-dependent manner (Rahman et al., 2007). As a first assay to establish auxinic activity of the 2,4-D analogues in our library (Figure 1), we tested the inhibitory effect of low (50 nM) and high (5 μM) concentrations on the primary root growth of Arabidopsis seedlings (Figure 3). Similar to 2,4-D, the compounds 4-Cl, 4-Br, 2-Cl-4-F, 2,4-DB, MCPA and Mecoprop inhibited the primary root elongation efficiently, both at low and high concentrations (Figure 3). Hence, we classified these compounds in one group called very active, appreciating that further confirmation by other assays (see below) is required to call them auxinic compounds.

Several compounds (4-F, 4-I, 2,5-D, 3,4-D, 2,4-Br, 2-F-4-Cl, 2-F-4-Br, 2,4,5-T, 2,4-DiB and 2,4-DP, MCPB) showed no inhibitory effect at 50 nM (Figure 3), whereas they exhibited a strong inhibitory effect at 5 μM (Figure 3). These compounds were classified as active. By contrast, 2-Cl, 2-I, 3-Cl, 2,6-D, 2,4-F, 2-NO_2-4-Cl, 2,3,4-T, 2,3,4-F, 2,4,6-T, 2,4,6-F, 2,4-DnP and 2,4-DnB had only a weak effect on root growth at 5 μM (Figure 3) and were therefore classified as weakly active. The remaining compounds PHAA, 2-F, 3-Me, 2,3-D, 3,5-M, 3-OMe, 4-NO_2, 3,5-Me, 3,5-D, 2-CL-4-Formyl, 2,4,6-T, and 2,4-DnP had no obvious inhibitory effect on root length, even at 5 μM (Figure 3), suggesting that these compounds have either very weak or no auxinic activity (Figure 3). For a complete overview of the 2,4-D analogues categorized based on their root growth inhibiting activity, the reader is referred to the supplementary data (Figure S2).

When establishing the root growth inhibition of our 2,4-D analogues, we observed that several compounds had a unique effect on the root system architecture (RSA). The analogues 2,5-D and 3-Cl strongly enhanced lateral and adventitious root formation while having an intermediate effect on root length (Figure S3), whereas 2,4,6-T, 3-Me, 2,3-D, 3,5-D and 2,4-DnP caused a reduction in the number of lateral roots without having a clear effect on root length (Figure S4). In addition, analogues 3-Cl, 3,4-D, 2,4-DP and Mecoprop were strong enhancers of root hair development (Figure S4). The above data indicate that specific 2,4-D analogues can be useful tools to predictably alter the RSA, as they have specific effects on root growth and development in a dose- and structure-dependent manner. Since the RSA is beyond the scope of this manuscript, we refer to the supplementary data for a more detailed description of our observations (Data S1).

The root growth inhibition by 2,4-D analogues corresponds to their auxinic activity

The *pDR5* promoter is a synthetic, generic auxin-responsive promoter that has been extensively used to visualize the cellular auxin response in Arabidopsis tissues (Ulmasov et al., 1997). To determine whether the root growth inhibition by 2,4-D analogues correlated with a molecular auxin response, we used an Arabidopsis line containing *pDR5* fused to a glucuronidase (GUS) reporter (*pDR5:GUS*). 2,4-D itself induced *pDR5* efficiently, as observed by a completely blue root following histochemical staining for GUS activity.

© 2023 The Authors.

1365313x, 2023, 5, Downloaded from https://onlinelibrary.wiley.com/doi/10.1111/tpj.16430 by University Of Leiden, Wiley Online Library on [28/11/2023]. See the Terms and Conditions (https://onlinelibrary.wiley.com/terms-and-conditions) on Wiley Online Library for rules of use; OA articles are governed by the applicable Creative Commons License

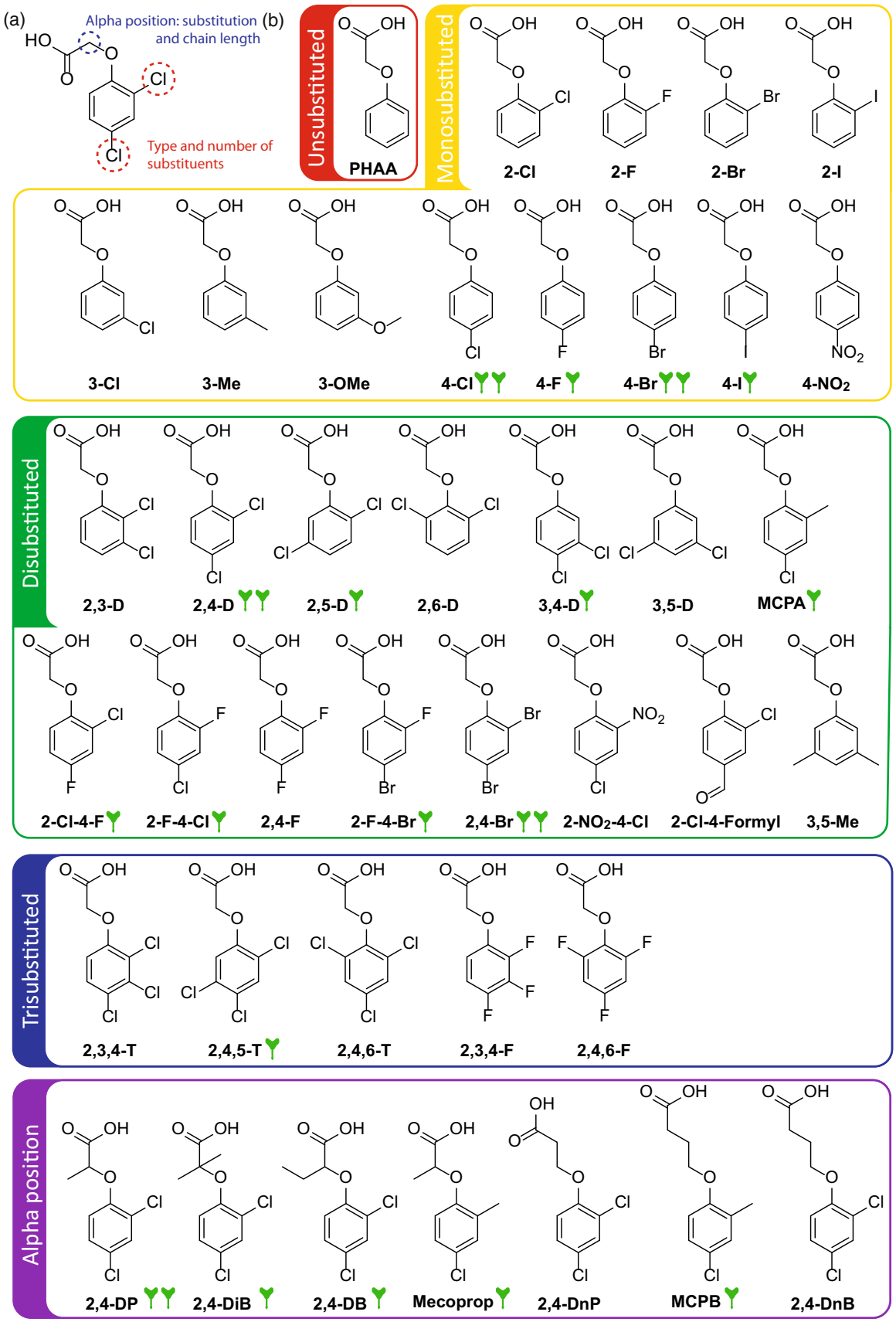

© 2023 The Authors.

1365313x, 2023, 5, Downloaded from https://onlinelibrary.wiley.com/doi/10.1111/tpj.16430 by University Of Leiden, Wiley Online Library on [28/11/2023]. See the Terms and Conditions (https://onlinelibrary.wiley.com/terms-and-conditions) on Wiley Online Library for rules of use; OA articles are governed by the applicable Creative Commons License

Figure 1. The composition of the 2,4-D analogue library.
(a) Structure of 2,4-D with the different modifications indicated that compose the 2,4-D analogue library.
(b) Structures of the 2,4-D analogues categorized based on the number of groups on the aromatic ring, or the substitution or chain length of the alpha position of the carboxylic acid side chain. Analogues that induced somatic embryogenesis efficiently or at a reduced efficiency are marked with (⚥⚥) or (⚥), respectively.

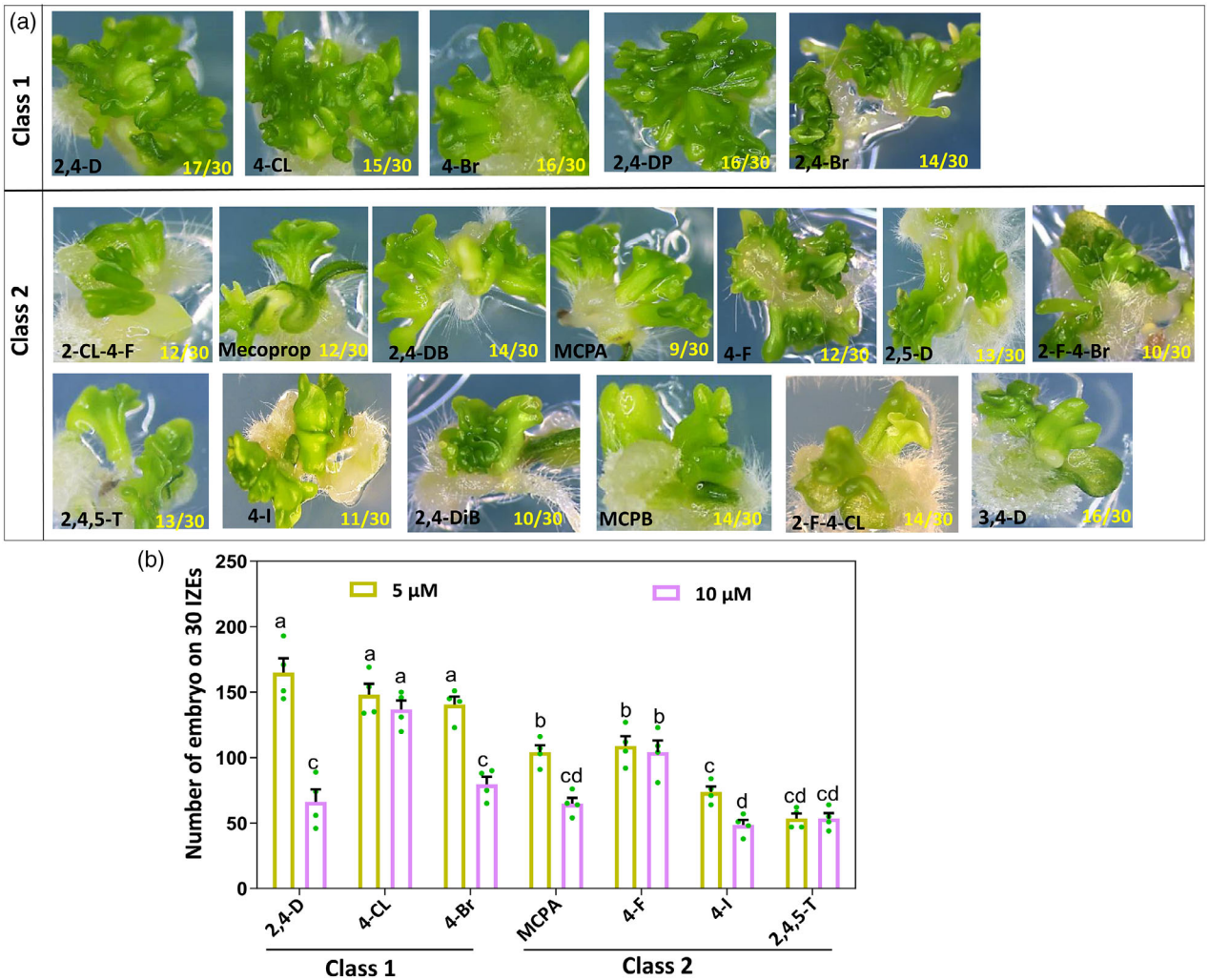

Figure 2. SE inducing capacity of 2,4-D analogues.
(a) The phenotype of somatic embryos formed on cotyledons of Arabidopsis IZEs that were first grown for 2 weeks in the presence of 5 µM 2,4-D or one of the 2,4-D analogues and subsequently cultured for 1 week on medium without any supplement. Class 1 compounds induced SE at the same efficiency as 2,4-D at a concentration of 5 µM and class 2 compounds do induce SE but are less effective.
(b) Quantification of the number of somatic embryos per 30 IZEs induced by 5 µM or 10 µM of 2,4-D or the indicated class 1 or class 2 2,4-D analogues. Dots indicate the number of somatic embryos produced per IZE ($n = 4$ biological replicates, with 30 IZEs per replicate), bars indicate the mean value and error bars of the SEM. Different letters indicate statistically significant differences ($P < 0.001$) as determined by one-way analysis of variance with Tukey's honest significant difference post hoc test. The structure of each compound is provided in Figure 1.

(Figure 4a). Because 2,4-D induced an especially strong *pDR5* activity in the cell division area of the root tip, we next quantified the effect of the 2,4-D analogues on *pDR5* activity in this part of the root tip (Figure 4b).

As expected, the compounds classified as very active (Figure S2) all strongly promoted *pDR5* activity in the cell elongation zone of Arabidopsis roots (Figure 4a,b), in line with their root growth inhibition activity. The *pDR5:GUS* expression was also clearly induced but varied more for the compounds classified as active (Figure 4a,b). For 2,5-D the induction of *pDR5:GUS* in the root meristem was not as high as for other active compounds, however, it did induce strong reporter expression in the differentiation zone of the root. The compounds that had only a slight effect on root growth and were therefore classified as weakly active, also only slightly promoted expression of the *pDR5:GUS* reporter in the root meristem (Figure 4a,b). Interestingly, like 2,5-D, 3-Cl induced a clear auxin

© 2023 The Authors.

1365313x, 2023, 5, Downloaded from https://onlinelibrary.wiley.com/doi/10.1111/tpj.16430 by University Of Leiden, Wiley Online Library on [28/11/2023]. See the Terms and Conditions (https://onlinelibrary.wiley.com/terms-and-conditions) on Wiley Online Library for rules of use; OA articles are governed by the applicable Creative Commons License

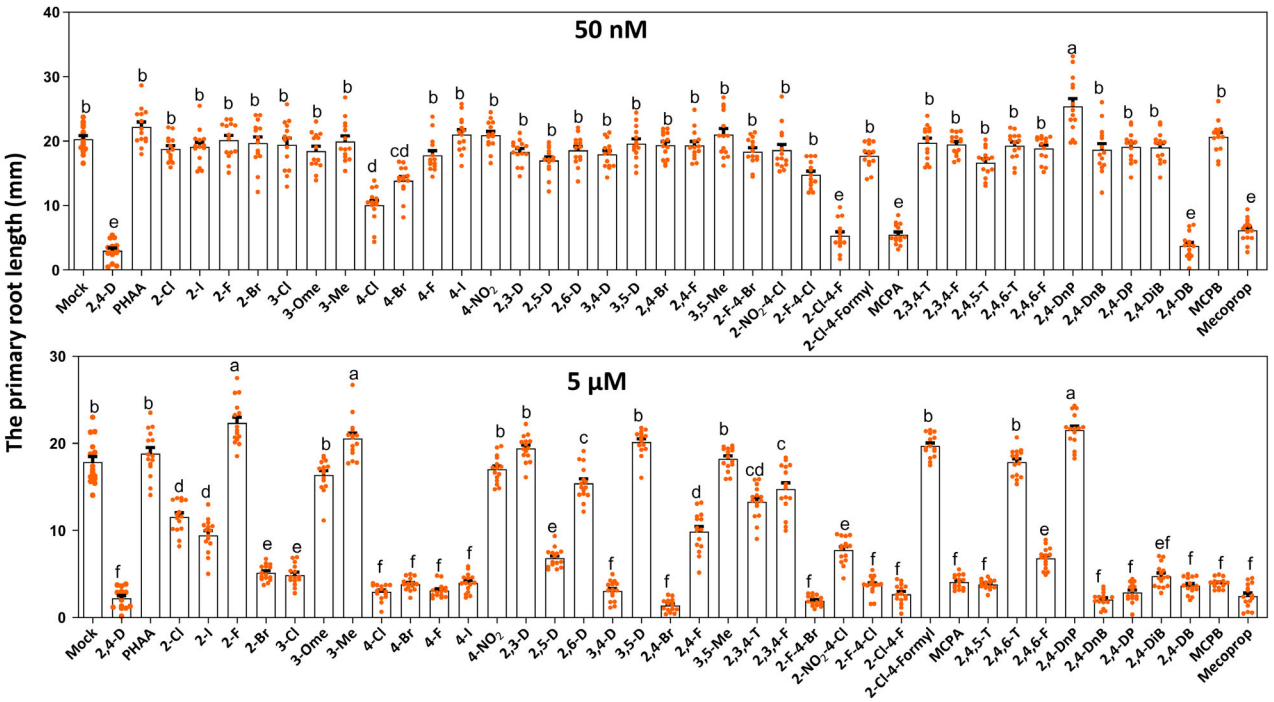

Figure 3. Effect of 2,4-D structure modifications on primary root growth inhibition in Arabidopsis. The primary root growth inhibition of seedlings grown in the presence of 50 nM (upper graph) and 5 µM (lower graph) of 2,4-D and 2,4-D analogues. Seedlings were first grown for 6 days on compound free-medium and subsequently transferred on medium with 2,4-D or a 2,4-D analogue for 3 days. Dots indicate the root length (mm) (n = 15 biological replicates), bars indicate the mean and error bars the s.e.m. and different letters indicate statistically significant differences ($P < 0.01$) as determined by a one-way analysis of variance with Tukey's honest significant difference post hoc test. The structure of each compound is provided in Figure 1.

response along the differentiation zone of the root (Figure 4a), something that was not observed for the other compounds classified as weakly active. The remaining library members that did not lead to inhibition of root growth also did not promote *pDR5* activity (Figure 4a,b). These findings show that the ability of the 2,4-D analogues to inhibit root growth correlates well with their auxinic activity (capacity to induce an auxin response).

To further confirm the auxinic activity of the 2,4-D analogues, we used the nuclear auxin input reporter R2D2, which acts as a proxy for the cellular sensing of auxin (Liao et al., 2015). The R2D2 reporter consists of two parts, an auxin-degradable DII domain fused to the yellow fluorescent nVENUS that is rapidly degraded when auxin concentrations increase as auxin sensor and an auxin-nondegradable DII domain (mDII) fused to the orange fluorescent nTdTOMATO as expression control (Liao et al., 2015). In accordance with observations based on *pDR5* activity, we detected strong down-regulation of the DII-nVENUS signal in the cell elongation zone of Arabidopsis roots treated with all very active and most of the active 2,4-D analogues (2,5-D, 3,4-D, 2,4-Br, 2-F-4-Br, 2,4-DP, and MCPB) and two weakly active compounds (2-Br and 2-NO2-4-Cl) (Figure S6). The other active and weakly active compounds elicited only moderate degradation of DII-Venus (Figure S6). The compounds that proved inactive as an auxin, as these did not inhibit root growth nor promoted *pDR5* activity, also did not lead to a detectable reduction of the DII-nVENUS signal in the cell elongation zone of roots (Figure S6). These results again supported the overall classification of the auxinic activity for our library of 2,4-D analogues (Figure S2).

Molecular dynamics simulations of binding of 2,4-D analogues to the TIR1-Aux/IAA coreceptors

Based on the combined results we classified all tested 2,4-D analogues from our library into five groups, namely very active, active, weakly active auxin analogues and not active and anti-auxin compounds (Figure S2). Our results show that the capacity of these auxin analogues to induce SE is tightly linked to their auxinic activity.

To correlate the auxinic activity of the 2,4-D analogues to their binding to the TIR1/AFB – Aux/IAA auxin co-receptors (Tan et al., 2007), we performed molecular dynamics (MD) simulations of this binding for a subset of 14 2,4-D analogues, representing derivatives from all auxinic activity classes, as determined in the *in planta* experiments. 2,4-D, IAA and NAA were taken along as controls (Figure 5). Among the library entries tested *in silico* are alpha-substituted compounds (methyl, ethyl or the Mecoprop derivatives 2,4-DP, 2,4-DB and Mecoprop, respectively) that due to their stereocenter can occur as the enantiomeric R or S stereoisomers. These compounds

© 2023 The Authors.

1365313x, 2023, 5, Downloaded from https://onlinelibrary.wiley.com/doi/10.1111/tpj.16430 by University Of Leiden, Wiley Online Library on [28/11/2023]. See the Terms and Conditions (https://onlinelibrary.wiley.com/terms-and-conditions) on Wiley Online Library for rules of use; OA articles are governed by the applicable Creative Commons License

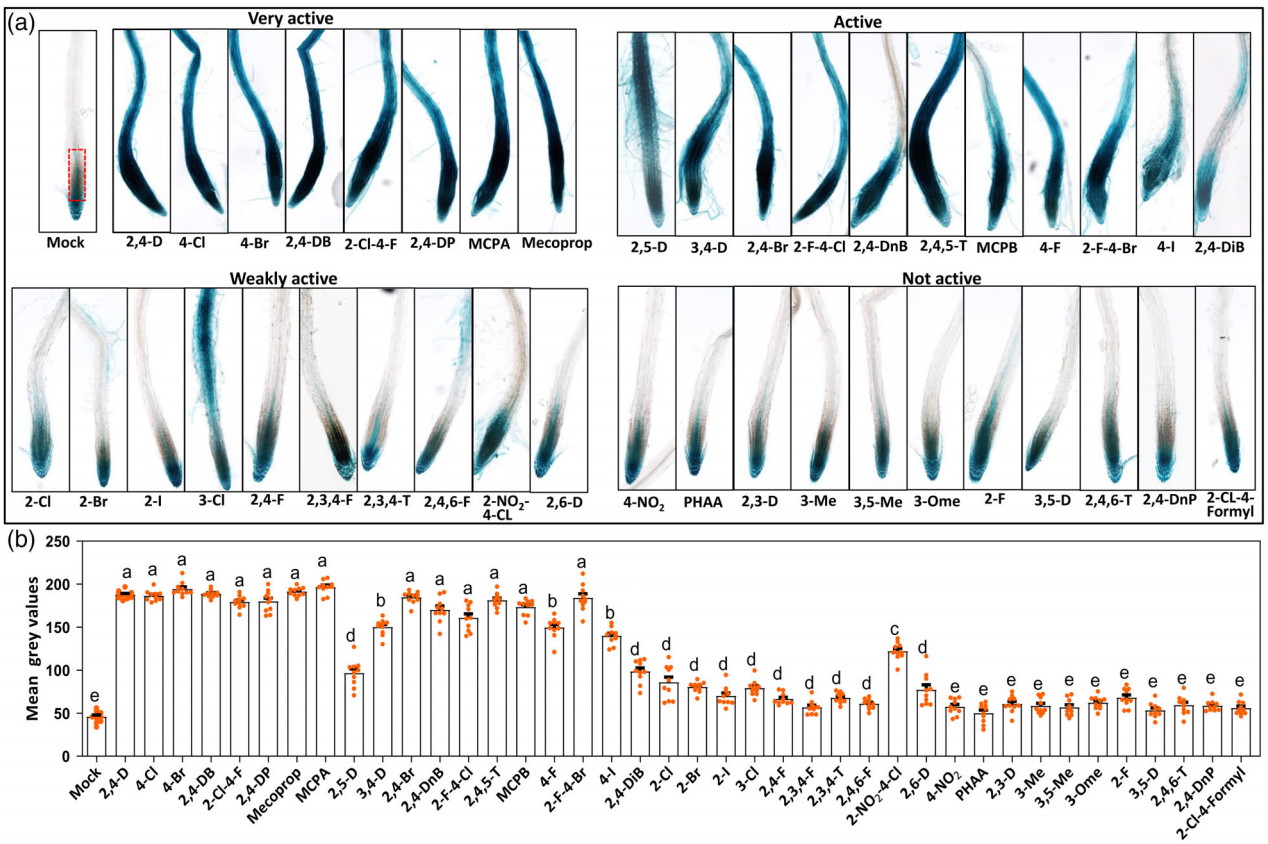

Figure 4. Auxin response induced by 2,4-D analogues.
(a) Expression of the auxin-responsive *pDR5:GUS* reporter in Arabidopsis seedling roots treated for 24 h with 5 μM of each 2,4-D analogue. For an overview of the 2,4-D analogues and their abbreviations, see Figure 1.
(b) Quantification of *pDR5:GUS* activity in the root meristems of Arabidopsis seedlings (region indicated with dotted red line in mock). Dots indicate the individual measurement of GUS activity staining per each treatment (n = 10 biologically independent seedlings per treatment, bars indicate the mean of each treatment and error bars the s.e.m. and different letters indicate statistically significant differences ($P < 0.01$) as determined by a one-way analysis of variance with Tukey's honest significant difference post hoc test. In A and B, seedlings were germinated for 6 days on compound-free medium, and for treatment, seedlings were transferred to a medium containing 5 μM of a 2,4-D analogue and incubated for 24 h.

were tested as mixture of these enantiomers in the *in planta* assays. The molecular dynamics simulation uniquely allowed us to investigate at a molecular level the potential differential binding of each enantiomer (notated as their acronym with an added R and S).

In the evaluation of the binding capacity of each auxin analogue within the system, we studied different aspects: the enthalpy of the system, the root-mean-square deviation (RMSD) of atomic positions of TIR1 along the simulation trajectory and the distance between the auxin analogue and the proline (7) of the Aux/IAA peptide (Figure 5). The RMSD of TIR1 reflects the system stability during the simulation. The last parameter, the distance (gamma) between the auxins analogue and the proline (7) of the Aux/IAA peptide, would show us which analogue is able to establish a CH·π interaction with the degron peptide that contributes to the binding interactions and thus to the stability of the complex (Wang & Yao, 2019). Our molecular dynamics simulations were based on a previously published method (Hao & Yang, 2010), but with a much longer trajectory of 200 ns instead of 2.5 ns.

The enthalpy was calculated using MMPBSA (Molecular Mechanics Poisson-Boltzmann Surface Area) with a lower enthalpy value indicating better binding. All the compounds classified as very active auxin analogues showed an enthalpy value below −12 Kcal/mol. Surprisingly, the weakly active 2,6-D and inactive 4-NO_2 were also in this range, suggesting that the binding enthalpy is not the sole parameter predictive for auxinic activity. The TIR1 protein RMSD calculation was carried out over the amino acids from position 50 till the end of the protein because the first 50 amino acids showed extra flexibility. The TIR1 N-terminal part is normally stabilized by the interaction with the SKP protein, which we did not include in our analysis. Moreover, this part does not interact with the auxin analogue nor with the AUX/IAA peptide and its structure has not been completely resolved in the employed crystal structure (Tan et al., 2007). All the compounds induced

© 2023 The Authors.

1365313x, 2023, 5, Downloaded from https://onlinelibrary.wiley.com/doi/10.1111/tpj.16430 by University Of Leiden, Wiley Online Library on [28/11/2023]. See the Terms and Conditions (https://onlinelibrary.wiley.com/terms-and-conditions) on Wiley Online Library for rules of use; OA articles are governed by the applicable Creative Commons License

Compound	Auxin activity†	Enthalpy binding (kcal/mol)	Distance gamma (Å)	Protein RMSD (Å)
2,4-D	very active	-26,9 ± 0,84	4,2 ± 0,38	1,4 ± 0,12
IAA	very active	-26,8 ± 0,80	4,0 ± 0,28	1,2 ± 0,13
NAA	very active	-29,6 ± 1,06	4,3 ± 0,39	1,6 ± 0,15
2,4-DB*(S)* *	very active	-30,8 ± 0,70	4,3 ± 0,33	1,3 ± 0,16
2,4-DB*(R)* *	very active	-29,3 ± 0,86	4,5 ± 0,45	1,3 ± 0,12
Mecoprop*(R)* *	very active	-26,7 ± 0,70	3,7 ± 0,3	1,5 ± 0,19
Mecoprop*(S)* *	very active	-15,1 ± 0,70	4,3 ± 0,36	1,3 ± 0,10
2,4-DP*(R)* *	very active	-25,1 ± 1,51	4,0 ± 0,37	1,5 ± 0,11
2,4-DP*(S)* *	very active	-22,4 ± 0,65	4,2 ± 0,33	1,2 ± 0,10
2-Cl-4-F	very active	-23,2 ± 0,81	4,0 ± 0,31	1,3 ± 0,12
4-Cl	very active	-13,0 ± 0,53	3,9 ± 0,28	1,4 ± 0,15
MCPA	very active	-12,8 ± 0,69	3,8 ± 0,29	1,4 ± 0,15
2,4-DiB	active	-19,5 ± 0,43	No CH·π	1,5 ± 0,14
3,4-D	active	-7,8 ± 0,54	4,0 ± 0,37	1,3 ± 0,09
2,6-D	weakly active	-36,5 ± 0,76	No CH·π	1,4 ± 0,13
2,3,4-T	weakly active	-8,8 ± 0,57	3,6 ± 0,23	1,2 ± 0,11
2,3,4-F	weakly active	-8,3 ± 0,67	4,2 ± 0,47	1,3 ± 0,11
4-NO2	not active	-13,6 ± 0,54	No CH·π	1,5 ± 0,23
2,4-DnP	anti-auxin	-8,4 ± 1,06	4,2 ± 0,57	1,1 ± 0,09
2,3-D	anti-auxin	-6,6 ± 0,69	4,2 ± 0,55	1,3 ± 0,13

Figure 5. Activity of auxins and 2,4-D analogues compared to the parameters from the molecular dynamics simulations for their binding to the TIR1-Aux/IAA coreceptors. †The auxins and 2,4-D analogues are ordered according to their established auxinic activity of the SAR (see also Figure S2). *These compounds were tested as a mixture of enantiomers in the planta assay, but separately in the MD simulations. Several parameters were calculated from the molecular dynamics simulations: (i) the enthalpy binding of the selected compounds and the standard deviation (std) was determined (kcal/mol), (ii) the distance between the gamma carbon of the proline of the AUX/IAA peptide and the ring mass centre of the compound and the corresponding standard deviation were determined (Distance gamma) (Å, at short distances, a stronger CH·π interaction is assumed) and (iii) the root-mean-square deviation of the TIR1 protein (Protein RMSD) with a standard deviation (std) was calculated as a measure of system stability during the simulation trajectory (Å). A larger distance (5 Å and more) the CH·π contribution is more or less negligible (No CH π). The colours (green to yellow) in the table are relative and indicate the match per parameter in the separate columns, and are a visual aid. The darker green indicates the better value, for example, 'dark' green in enthalpy binding indicates the compound is a better binder considering enthalpy than other compounds in the table.

similar RMSD values of the TIR1 protein ranging from 1.1 to 1.6, indicating that binding to the compounds tested does not induce significant differences in the stability of the protein backbone (Figure 5). Finally, we observed the proximity between the proline (7) from the AUX/IAA peptide and the 2,4-D analogue, so we monitored this distance along the simulation trajectory for all the derivatives. The distance was measured specifically between the gamma carbon of proline (7) and the ring mass centre of the auxin analogue (distance gamma) (Figure S7), assuming that a shorter distance would predict a stronger CH·π interaction (Wang & Yao, 2019). Compounds 4-NO_2 (5,3 Å) and 2,6-D (5,0 Å) showed the two largest distances at which the CH·π contribution is more or less negligible, explaining why these compounds are weakly active or inactive despite their low enthalpy. For IAA and the very active 2,4-D analogues distance values varied between 3,7 Å (Mecoprop) and 4,5 Å (2,4-DB(R)). Several weakly active and anti-auxin compounds were also in this range. However, as the binding enthalpy was above −12 Kcal/mol, this would explain why these compounds lacked auxinic activity.

SE and stress responses induced by 2,4-D are both downstream of auxin signalling

The above data indicated that there is a strong correlation between auxinic activity, simulated co-receptor binding and SE induction: SE is only obtained with the 2,4-D analogues that induce a strong to very strong auxin response

© 2023 The Authors.

1365313x, 2023, 5, Downloaded from https://onlinelibrary.wiley.com/doi/10.1111/tpj.16430 by University Of Leiden, Wiley Online Library on [28/11/2023]. See the Terms and Conditions (https://onlinelibrary.wiley.com/terms-and-conditions) on Wiley Online Library for rules of use; OA articles are governed by the applicable Creative Commons License

and the compounds inducing a very strong auxin response are generally more efficient in inducing SE than the ones inducing a strong response (Figures 2–4 and Figure S2). This led us to hypothesize that (i) 2,4-D and its analogues induce SE through the canonical TIR1/AFB co-receptor-triggered auxin signalling pathway, and that (ii) the stress response required for SE induction (Jin et al., 2014; Mantiri et al., 2008; Nowak et al., 2015; Salvo et al., 2014) is the result of the strong auxin response induced by 2,4-D and its analogs.

To test the first hypothesis, we used Arabidopsis *tir1*, *afb1*, *afb2*, *afb3*, *afb4* and *afb5* single mutants and double, triple and quadruple mutant combinations that showed clear rosette and inflorescence phenotypes but still allowed embryo development and seed set (Prigge et al., 2020) in 2,4-D induced SE experiments. Four of the single mutants and the two double mutant combinations only showed a mild but significant reduction of around 30% in SE efficiency, but the efficiency was strongly reduced (66%) in the *tir1 afb2 afb3* triple and the *tir1 afb2 afb4 afb5* quadruple, and an even more strong reduction (80%) was observed with the *tir1 afb1 afb2 afb3* quadruple mutant (Figure 6). The results confirm our hypothesis that 2,4-D induces SE via the canonical auxin response pathway, and also suggest that there are no 2,4-D specific co-receptors and that the members of the TIR1/AFB family act

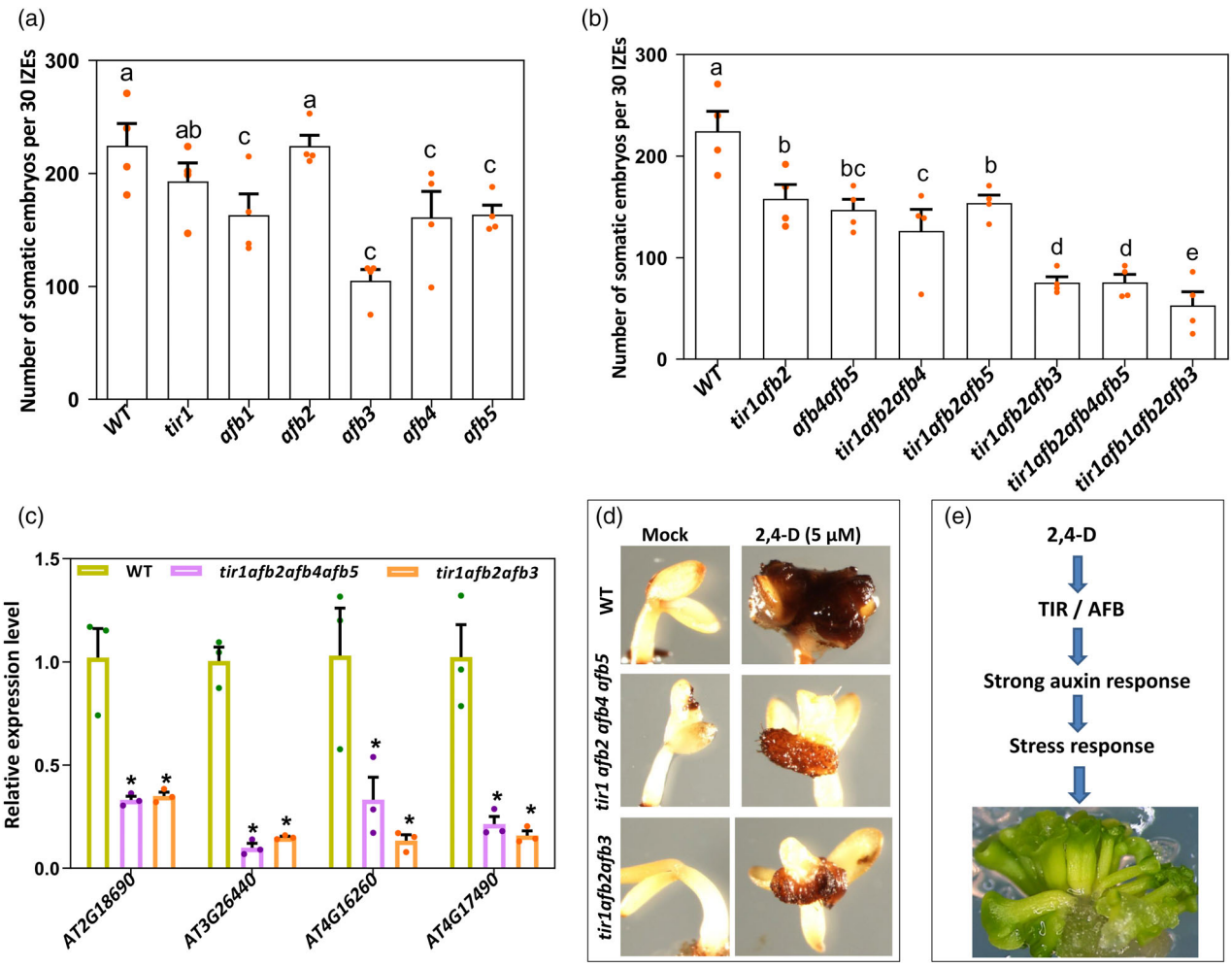

Figure 6. Induction of SE or stress responses by 2,4-D requires the canonical auxin signalling pathway (a, b) Efficiency of SE induced by 2,4-D treatment on immature embryos of Arabidopsis wild type (Col-0, WT) or different single (a) or double, triple or quadruple mutants (b). Dots indicate the number somatic embryos produced per 30 IZEs ($n = 4$ biological replicates), bars indicate the mean value and error bars the SEM. Different letters indicate statistically significant differences ($P < 0.01$) as determined by one-way analysis of variance with Tukey's honest significant difference post hoc test. (c) Induction of expression of four general stress-induced genes in wild-type (WT, Col-0) or *tir1 afb* triple or quadruple mutant immature zygotic Arabidopsis embryos cultured for 7 days on medium without 2,4-D. Dots indicate the values of three biological replicates per plant line, bars indicate the mean and error bars indicate s.e.m. Asterisks indicate significant differences from WT ($P < 0.01$), as determined by a two-sided Student's *t*-test. (d) Induction of reactive oxygen species (hydrogen peroxide) marked by the brown polymerization product of diaminobenzidine tetrahydrochloride after 7 days of 2,4-D treatment in wild-type (WT, Col-0) or *tir1 afb* triple or quadruple mutant immature zygotic Arabidopsis embryos. (e) Model for 2,4-D-induced SE: 2,4-D is perceived by the canonical TIR1/AFB auxin receptors and the resulting strong auxin response, which includes stress signalling required for the induction of somatic embryos.

© 2023 The Authors.

1365313x, 2023, 5, Downloaded from https://onlinelibrary.wiley.com/doi/10.1111/tpj.16430 by University Of Leiden, Wiley Online Library on [28/11/2023]. See the Terms and Conditions (https://onlinelibrary.wiley.com/terms-and-conditions) on Wiley Online Library for rules of use; OA articles are governed by the applicable Creative Commons License

redundantly in this process, even AFB5 that was reported not to show enhanced 2,4-D insensitivity and instead to be specific for pyridinecarboxylic acid type herbicides (Walsh et al., 2006).

To test the second hypothesis, we used four stress reporter genes (see Appendix S1 for more information) and staining for reactive oxygen species (ROS). In the *tir1 afb2 afb3* triple and the *tir1 afb2 afb4 afb5* quadruple mutants, induction of the stress reporter genes by 2,4-D was strongly reduced and no staining of ROS was observed as compared to the wild-type control (Figure 6). The results confirm our hypothesis that the 2,4-D induced stress responses are downstream of the canonical auxin signalling pathway.

DISCUSSION

Chemical biology has been instrumental in enhancing our understanding of auxin biology, as several key molecules that are currently used to specifically modulate auxin biosynthesis, signalling or transport have been identified in chemical genetic screens (Ma et al., 2018; Simon et al., 2013). 2,4-D is a synthetic auxin that is widely used as a herbicide, but also as a plant growth regulator in *in vitro* regeneration and auxin research (Peterson et al., 2016; Skůpa et al., 2014). In this study, 2,4-D analogues with varying modifications, including the type and number of substitutions on the aromatic ring (like chlorine, bromine, fluorine, iodine, nitro, methyl group) or substitutions on or elongation of the alpha-position (Figure 1) have been evaluated for their structure–activity relationship and ability to induce SE.

The capacity of SE induction by 2,4-D analogues

SE is experimentally induced by application of exogenous plant growth regulators under *in vitro* conditions (Nic-Can et al., 2015). 2,4-D is the most well-known plant growth regulator that is widely used for SE. Our screen revealed four 2,4-D analogues (4-Cl, 4-Br, 2,4-DP, and 2,4-Br) that also efficiently induce SE from Arabidopsis IZEs, whereas 13 analogues (4-F, 4-I, 2,5-D, 3,4-D, 2-F-4-Cl, 2-F-4-Br, 2,4,5-T, 2,4-DiB, MCPB, MCPA, and Mecoprop) induced SE at a lower efficiency (Figure 2 and Figure S1). Except for 3,4-D and 2,4,5-T, which have been shown to efficiently induce SE in other plant species (Kouassi et al., 2017), SE induction by the other 2,4-D analogues has not been reported before. We did not identify a 2,4-D analogue with enhanced capacity to induce SE, suggesting that for our system 2,4-D is still the best compound to use. However, since 2,4,5-T efficiently induces SE in other plant species but less efficiently in Arabidopsis, it is to be expected that some of the 2,4-D analogues presented here might be used to establish an efficient SE system in other plant species. Moreover, 2,4-D treatment has been reported to lead to a significant percentage of abnormal somatic embryos in many plant species (Garcia et al., 2019). The use of the 2,4-D analogues identified here may reduce the number of abnormal embryos, but this still requires testing in the different SE systems.

We also showed that only 2,4-D analogues that classify as very active or active auxinic compounds are able to induce SE from Arabidopsis IZEs, which indicates that the capacity to induce SE is primarily linked to auxinic activity. Stress has also been identified as an important factor in SE induction (Jin et al., 2014; Mantiri et al., 2008; Nowak et al., 2015; Salvo et al., 2014). Our 2,4-D analogue screen together with the strong reduction in SE and stress responses in *tir/afb* triple and quadruple mutants suggest that in our SE system stress is downstream of auxin signalling, and not a parallel pathway that is additionally triggered by 2,4-D or its analogues. It is therefore unlikely that a chemical biology approach as presented here will allow us to tease apart the stress and auxin pathways by identifying compounds that trigger each pathway separately. The new 2,4-D analogues identified here can be useful tools to study the importance of aspects of auxin physiology either during SE induction or through their effects on the root system architecture. For example, it would be interesting to understand why MCPA, which is classified as a very active auxin, based on root growth inhibition and auxin response reporter expression, shows a significantly reduced capacity to induce SE. And why does 3-Cl, classified as weakly active auxin, strongly induce the auxin response in the root differentiation zone thereby specifically promoting root hair formation? Or how can 3,5-D strongly inhibit lateral root formation without clearly affecting auxin-responsive gene expression? These differences may lie in the compound-specific metabolism or transport characteristics of the 2,4-D analogues, which have already been shown to differ between the natural auxin IAA and the synthetic auxins 2,4-D and 1-NAA (Delbarre et al., 1996; Eyer et al., 2016; Song, 2014).

Auxinic activity of 2,4-D analogues correlates to simulated binding properties to TIR1

The Arabidopsis seedling root growth inhibition assay combined with the use of the *pDR5:GUS* and *R2D5* auxin response reporters provided consistent results with respect to classifying the 40 2,4-D orthologs as very active, active or weakly active auxin analogues, or having no auxin or possibly anti-auxin activity. Importantly, this classification was in agreement with previously published results on the 2,4-D analogues PHAA (inactive), 2,4 Br, 2,4,5-T, 3-Me, 2,4-DP and MCPB (Simon et al., 2013; Torii et al., 2018). This difference in auxinic activity is clearly determined by structure and chemical properties of these compounds, which relates on the one hand to their binding affinity to the TIR1/AFB (Calderón Villalobos et al., 2012) and AUX/IAA (Torii et al., 2018) co-receptor pair, and on the other hand to their transport or conjugation properties or metabolic decay in plant cells. For example, 2,4-D itself it has been shown to be

© 2023 The Authors.

1365313x, 2023, 5, Downloaded from https://onlinelibrary.wiley.com/doi/10.1111/tpj.16430 by University Of Leiden, Wiley Online Library on [28/11/2023]. See the Terms and Conditions (https://onlinelibrary.wiley.com/terms-and-conditions) on Wiley Online Library for rules of use; OA articles are governed by the applicable Creative Commons License

conjugated to Asp and Glu, and the conjugates still display residual auxinic activity (Eyer et al., 2016).

Molecular dynamics simulations indicated that the auxinic activity of most 2,4-D analogues could be correlated to their binding strength to TIR1. One important factor here was the theoretical enthalpy of the system, as all very active auxin analogues showed an enthalpy value below −12 Kcal/mol. However, the distance between Pro7 of Aux/IAA and the 2,4-D analogue was also important, as some of the tested analogues lacking this CH·π interaction showed no or only weak auxinic activity, despite the fact that their enthalpy value was below −12 Kcal/mol.

It is important here to note two things regarding the MD simulations. First, although the results from MD simulation are generally well in accordance with the observed auxinic activity, we cannot account for uptake, efflux, transport and metabolism of the compound in the simulations. And second, due to the expensive cost of entropy calculation combined with low reliability for such a big system, we did not calculate this parameter. However, we considered that the molecules are very similar and, although we know there will be differences in entropy among the derivatives, we assume that they will not change the results dramatically.

Structure–activity relationship of 2,4-D analogues based on auxinic activity

Among the 40 compounds in our screen, several have previously been tested for auxinic activity, based on wheat coleoptile elongation, pea stem curvature, tomato leaf epinasty, root growth inhibition and/or root or callus induction (Ferro et al., 2007, 2010; Hayashi et al., 2012; Katekar, 1979; Koepfli et al., 1938; Lee et al., 2014; Quareshy et al., 2018; Song, 2014; Tan et al., 2007). As pointed out in the introduction and results sections, comparing auxinic activity with these previous studies is difficult because of these different assay types, or possibly impure compounds (Ferro et al., 2007). Our study is unique in that we first assembled an extensive collection of commercially available and tailor-made compounds that provide a rational coverage of possible 2,4-D analogues and verified their purity by Nuclear Magnetic Resonance spectroscopy. We then evaluated and compared these compounds in terms of physiological root growth inhibition response and auxin response reporters during auxinic activity tests. Assuming that the auxin response reporters are the most direct and universal indicators of auxinic activity and that 2,4-D analogues are stable and there is no change in activity during the assay due to compound metabolization, we summarize several trends for the structure auxinic activity relationship of 2,4-D analogues based on the set of 40 tested here. First, a halogen at the 4-position is more important for auxinic activity than at the 2-position (4-Cl; 2-Cl-4-F; 4-I/Br/F; versus 2-Cl/I/Br/F). Second, the activity of analogues with a substitution at the 3- or 5- position remains, but such compounds are less active compared to 2,4-substitutions (2,5-D; 3,4-D; 2,4,5-T). Third, both substitutions at the alpha position (Mecoprop; 2,4-DP; 2,4-DB; 2,4-DiB) and a longer carboxylate chain with an even number of carbons are tolerated (MCPB; 2,4-DnB). This latter finding is in agreement with a previous study that showed that IAA analogues with a substitution on their carboxylate chain, up to $n = 4$ carbons, can still bind to TIR1, thus allowing for a modification on this position (Hayashi et al., 2008). Taken these trends together, we conclude that an electron-withdrawing group, in particular a halogen, at the 4-position is important for auxinic activity. In addition, we suggest that electron withdrawing or donating properties of the 2-position are less important for auxinic activity and that the size of the 2-substituent could influence auxinic activity, since both methyl and chloro groups are accepted at this position (like 2,4-D and MCPA). There is, however, an outlier based on this general conclusion: 2,4-F is only weakly active but has a strong electron withdrawing group at the 4-position. Altogether, these results indicate that small modifications at different parts of 2,4-D can lead to different physiological activities, generating molecules with interesting other applications in plant (tissue) culture than SE, as described below.

Several 2,4-D analogues are useful tools to modulate the root system architecture

In the assessment of 2,4-D analogues, we have found that some 2,4-D analogues (2,3-D, 3,5-D, 3-Me, 2,4,6-T and 2,4-DnP) either had no effect on or only slightly affected root growth (Figure 3), whereas they inhibited the formation of lateral roots (Figure S5). Since inhibition of lateral root formation is typical for compounds with anti-auxin activity (Larsen, 2017), we suspected that they may act as anti-auxins. Such anti-auxin activity could be caused by high affinity binding to only one of the co-receptors, thereby preventing the formation of the F-box-Aux/IAA complex. As such, high concentrations of an anti-auxin would compete effectively with IAA for establishing the TIR1-Aux/IAA complex required for ubiquitination-mediated degradation of the Aux/IAA repressors. Interestingly, our 2,4-D analogues did not change *pDR5* activity, nor did they lead to enhanced or reduced degradation of DII-VENUS in the root tip, which would be expected for an anti-auxin. Moreover, the negative effect on lateral root formation varied per compound. For example, 3-Me only mildly affected lateral root formation, whereas 3,5-D and 2,4-DnP almost completely inhibited this process, with 3,5-D preferably blocking at stage 2 (enhanced number of stage 2 primordia) whereas 2,4DnP resulted in a reduction of all stages. Clearly, further research on these 2,4-D analogues, such as a forward genetic screen for mutants that develop lateral roots when grown on the compound, is required to unravel the exact molecular mechanism by which they repress

© 2023 The Authors.

1365313x, 2023, 5, Downloaded from https://onlinelibrary.wiley.com/doi/10.1111/tpj.16430 by University Of Leiden, Wiley Online Library on [28/11/2023]. See the Terms and Conditions (https://onlinelibrary.wiley.com/terms-and-conditions) on Wiley Online Library for rules of use; OA articles are governed by the applicable Creative Commons License

lateral root formation. As such, these 2,4-D analogues could uncover new components involved in lateral root formation. At the same time, they could be used to modulate lateral root formation, e.g. to prevent branching during early seedling development to obtain a deeper root system.

Adventitious root (AR) formation is an organogenesis process by which new roots are produced from non-root tissues. AR induction is an important but often rate-limiting step in the vegetative propagation of many horticultural and forestry plant species. Generally, AR induction is promoted by auxins, and IBA and NAA are the most common auxins used for this purpose in commercial operations (Geiss et al., 2009). Our results show that 2,5-D and 3-Cl efficiently induce ARs from Arabidopsis hypocotyls, even more efficiently than IBA or NAA. Therefore, 2,5-D and 3-Cl are recommended as new AR inducers and they may be used to resolve rooting in recalcitrant species.

Roots hairs extend from root epidermal cells in the differentiation zone of the root and support plants in nutrient absorption, anchorage, and microbe interactions (Lee & Cho, 2013). Exogenous auxin treatments generally promote root hair induction and development (Lee & Cho, 2013). We showed that some 2,4-D analogues (3-Cl, 3,4-D, 2,4-DP, and Mecoprop) induced ectopic root hair formation on Arabidopsis roots, while promoting lateral root formation and having a relatively mild effect on root growth compared to 2,4-D itself. Specifically, roots of plants grown on the analogue 3-Cl produced several times more root hairs compared to other analogues. Unlike other 2,4-D analogues, 3-Cl specifically induced a strong auxin response in the differentiation zone of the root and a weaker response in the root elongation zone (Figure 4). This could explain the differential effect of 3-Cl on root biomass. We recommend 3-Cl as a promising compound for use in horticulture or agriculture to enhance root hair formation and thereby improve crop performance by enhanced ion and water uptake.

EXPERIMENTAL PROCEDURES

2,4-D and 2,4-D-analogues

The 2,4-D analogues that were used in this study were divided into 2 main categories. The first one contained 2,4-D analogues with substituents at different positions on the aromatic ring (Figure 1). The second group consisted of 2,4-D analogues with different carbon chains at the alpha-position of 2,4-D. (Figure 1). The reader is kindly referred to the Supplementary Information for more information on sources for commercially available compounds (Appendix S2), the synthesis of certain library members (Appendix S3) and NMR spectra of the compounds indicating their purity (Appendix S4).

The acronyms of the 2,4-D analogues were assigned based on established acronyms in literature, or based on the number and substitution type on the aromatic ring, or the type of substituent on the alpha position of the carboxylate.

Plant materials and growth conditions

This research used *Arabidopsis thaliana* Columbia-0 (Col-0) wild type, and the *pDR5::GUS* (Benjamins et al., 2001) and *R2D2* (Liao et al., 2015) reporter lines in the Columbia background. Arabidopsis *tir1*, *afb1*, *afb2*, *afb3*, *afb4* and *afb5* single mutants and the *tir1 afb2* and *afb4 afb5* double, *tir1 afb1 afb2* and *tir1 afb2 afb4* triple and *tir1 afb1 afb2 afb3* and *tir1 afb2 afb4 afb5* quadruple mutant combinations have been described previously (Prigge et al., 2020). For *in vitro* plant culture, seeds were sterilized in 10% (v/v) sodium hypochlorite for 10 min and then 4 times washed with MQ water. Sterilized seeds were plated on ½ MS medium and grown in the tissue culture room at 21°C, 16 h photoperiod and 50% relative humidity. After around 2 weeks, the germinated seeds were planted in soil in the climate room at 20°C, 16 h photoperiod and 70% relative humidity.

Arabidopsis primary root growth assay adventitious root induction

The Arabidopsis seeds were germinated on ½ MS medium. Five-day-old seedlings were transferred to new ½ MS medium supplemented with 2,4-D analogues. The length of the primary root was quantified after 3 days, incubation with 2,4-D analogues. Primary root length and lateral root numbers were analyzed with ImageJ software.

For the adventitious root (AR) induction, the seed was first grown in complete darkness. Six-day-old seedlings were transferred to new ½ MS medium supplemented with 2,4-D analogues 16 h photoperiod. The number of ARs induced from hypocotyls was quantified after 7 days.

Histochemical staining assays

In order to test auxinic activity of 2,4-D analogues, the activity *pDR5:GUS* auxin response reporter was investigated in the presence of 5 μM of each analogue. Histochemical β-glucuronidase (GUS) staining was performed as described previously (Anandalakshmi et al., 1998) with some modifications. Samples were submerged in 1-2 ml staining solution and incubated for 4 h at 37°C followed by rehydration.

Reactive oxygen species (H_2O_2) was detected by staining 3,3′-diaminobenzidine tetrachloride (DAB) (Fryer et al., 2002). Samples were submerged in 0.05% DAB solution for 6 h in the dark at room temperature. Samples incubated in DAB were rinsed with distilled water and then mounted on slides for light microscope.

qPCR analysis

RNA was isolated from lZEs cultured on B5 medium with or without 2,4-D using the RNEasy© kit (Qiagen, Venlo, Netherlands). First-strand cDNA was synthesized using the RevertAid RT Reverse Transcription kit (Thermo Fischer Scientific, Waltham, Massachusetts, US). Quantitative PCR was performed on three biological replicates along with three technical replicates using the SYBR-green dye premixed master mix (Thermo Fischer Scientific) in a C1000 Touch© thermal cycler (BIO-RAD, Veenendaal, Netherlands). CT values were obtained using Bio-Rad CFX manager 3.1. The relative expression level of genes was calculated according to the $2^{-\Delta\Delta Ct}$ method (Livak & Schmittgen, 2001). Expression was normalized using the *BETA-6-TUBULIN* (*TUB6*) gene as reference. The primers used are described in Table S1.

Somatic embryogenesis induction

For SE induction, 11 days old siliques of Arabidopsis Columbia-0 wild-type were sterilized in 10% (v/v) sodium hypochlorite for

© 2023 The Authors.

1365313x, 2023, 5, Downloaded from https://onlinelibrary.wiley.com/doi/10.1111/tpj.16430 by University Of Leiden, Wiley Online Library on [28/11/2023]. See the Terms and Conditions (https://onlinelibrary.wiley.com/terms-and-conditions) on Wiley Online Library for rules of use; OA articles are governed by the applicable Creative Commons License

10 min and then washed with MQ water for 4 times. Sterilized siliques were dissected to acquire IZEs. IZEs were cultured on B5 medium mixed with 2,4-D analogues for 14 days in the culture room at 21°C, 16 h photoperiod and 50% relative humidity. The IZEs were then transferred to ½ MS medium for 7 days and the number of SEs was counted under a light microscope. The quality of the obtained SEs was then further examined by moving embryos to the MS media in square petri dishes. Some 2,4-D analogues inactive in inducing SE were combined with IAA or NAA. In this experiment, B5 medium supplemented with 2,4-D was used as a control.

Microscopy

GUS-stained tissues were observed and photographed using a Nikon Eclipse E800 microscope. Cellular and subcellular localization of DII-VENUS and TdTOMATO proteins was visualized by confocal laser scanning microscope (ZEISS-003-18 533) using a 534 nm laser combined with a 488 nm LP excitation and 500–525 nm BP emission filters for DII-VENUS signals or 633 laser and 532 nm LP excitation and 580–600 nm BP emission filters for TdTOMATO signals.

Molecular dynamics simulations

Molecular dynamics simulations (see Methods S1 for protocol) were run using the crystal structure of the systems comprising the TIR1, auxin-responsive protein fragment, co-factor inositol hexakisphosphate, and the auxin. In particular, the structure deposited in the PDB under the ID 2P1N (Tan et al., 2007) was used as a starting structure. The auxin derivative was replaced by the different auxin candidates before running the MD simulations. Both the system preparation and the simulations were performed in the AMBER 18 suite software (Case, 2018). An updated version of the protocol described in Hao and Yang's article was used (Hao & Yang, 2010). Firstly, the system is neutralized by adding sodium ions and later fitted into a cubic box using TIP3P water parameters (Mol. Phys, 1988, 94, 803–808). The cubic box is built by placing the protein into the box centre and expanding the box size with 10 Å at the edge of the protein in each direction. The force fields used to obtain topography and coordinates files were ff14SB (Maier et al., 2015) and GAFF (Wang et al., 2004). The first step of the protocol (see supporting info for detailed parameters employed) followed to run the MD simulations is a minimization only of the positions of solvent molecules keeping the solute atom positions restrained and, the second stage minimizes of all the atoms in the simulation cell. Heating the system is the third step raising gradually the temperature from 0 to 300 K under a constant volume and periodic boundary conditions. In addition, Harmonic restraints of 10 kcal·mol^{-1} were applied to the solute, and the Berendsen temperature coupling scheme (Berendsen et al., 1984) was used to control and equalize the temperature. The time step was kept at 2 fs during the heating phase. Long-range electrostatic effects were modelled using the particle-mesh-Ewald method (Darden et al., 1993). The Lennard-Jones interactions cut-off was set at 8 Å. An equilibration step for 100 ps with a 2 fs time step at a constant pressure and temperature of 300 K was performed prior to the production stage. The trajectory production stage kept the equilibration step conditions and was prolonged for 200 ns longer at the 1 fs time step. Besides, the auxin analogues required a previous preparation step where the parameters and charges were generated by using the antechamber module of AMBER, using the GAFF force field and AM1-BCC method for charges (Jakalian et al., 2002). In addition, 100 frames evenly separated during the last 5000 steps of the simulation were employed for the enthalpy calculation by using MM-PBSA approximation. The following cpptraj modules were employed to analyse and harvest the data:

- rms module for RMSD calculation on the protein backbone (C, CA, N).
- Distance module for proline auxin distance CH·pi interaction.
- Angle module for angle for CH·pi interaction.
- trajout output pdb multi command to extract frames.

ACCESSION NUMBERS

TIR1: *At3g62980*, *AFB1*: *At4g03190*, *AFB2*: *At3g26810*, *AFB3*: *At1g12820*, *AFB4*: *At4g24390*, *AFB5*: *At5g49980*, *At2g18690*, *At3g26440*, *At4g16260*, *ERF6: At4g17490*, *TUB6*: *At4g14960*.

ACKNOWLEDGEMENTS

The *tir/afb* single mutants and the double, triple and quadruple mutant combinations were kindly provided by M Prigge and M. Estelle. This publication was part of the project StressAuxEmb (with project number 737.016.013) of the research programme Building Blocks of Life, which was (partly) financed by the Dutch Research Council (NWO). Victor J Somovilla is thankful for the financial support to EU Commission (Marie Skłodowska-Curie 840663 to V.J.S.) and Maria de Maeztu Units of Excellence Programme – Grant No. MDM-2017-0720 Ministry of Science, Innovation and Universities.

CONFLICTS OF INTEREST

The authors declare no competing financial interests.

AUTHOR CONTRIBUTIONS

OK, HJ and VJS: Methodology, Formal analysis and Validation. OK, HJ, VJS, BVA, ABS, MH, and AK: Investigation. OK, HJ, TW and RO: Conceptualization and Writing – Original Draft. All authors: Writing – Review & Editing. TW and RO: Supervision and Funding Acquisition.

DATA AVAILABILITY STATEMENT

All data supporting the findings of this study are available within the paper and within the supplementary data published online. Raw data are available from the corresponding author, (Remko Offringa), upon request. Novel materials used and described in the paper are available upon request for non-commercial research purposes.

SUPPORTING INFORMATION

Additional Supporting Information may be found in the online version of this article.

Data S1. 2,4-D analogues and root system architecture

Figure S1. 2,4-D analogues that do not induce SE.

Figure S2. The library of 40 2,4-D analogues used in this study.

Figure S3. Certain 2,4-D analogues specifically promote root hair formation.

Figure S4. Efficient lateral and adventitious root induction by specific 2,4-D analogues.

© 2023 The Authors.

1365313x, 2023, 5, Downloaded from https://onlinelibrary.wiley.com/doi/10.1111/tpj.16430 by University Of Leiden, Wiley Online Library on [28/11/2023]. See the Terms and Conditions (https://onlinelibrary.wiley.com/terms-and-conditions) on Wiley Online Library for rules of use; OA articles are governed by the applicable Creative Commons License

Figure S5. Several 2,4-D analogues inhibit lateral root formation in Arabidopsis.

Figure S6. R2D2-reported auxinic activity of the 40 2,4-D analogues

Figure S7. CH·pi interaction between 2,4-D and proline during the MD simulations.

Method S1. Protocol for molecular dynamics simulations.

Table S1. Primers used for qRT-PCR

Appendix S1. Stress reporter genes.

Appendix S2. A list of commercially available 2,4-D analogues.

Appendix S3. Chemical synthesis of 2,4-D analogues.

Appendix S4. NMR spectra.

REFERENCES

Anandalakshmi, R., **Pruss, G.J.**, **Ge, X.**, **Marathe, R.**, **Mallory, A.C.**, **Smith, T.H. *et al.*** (1998) A viral suppressor of gene silencing in plants. *Proceedings of the National Academy of Sciences of the United States of America*, **95**, 13079–13084.

Benjamins, R., **Quint, A.**, **Weijers, D.**, **Hooykaas, P.** & **Offringa, R.** (2001) The PINOID protein kinase regulates organ development in Arabidopsis by enhancing polar auxin transport. *Development*, **128**, 4057–4067.

Berendsen, H.J.C., **Postma, J.P.M.**, **van Gunsteren, W.F.**, **DiNola, A.** & **Haak, J.R.** (1984) Molecular dynamics with coupling to an external bath. *The Journal of Chemical Physics*, **81**, 3684–3690.

Calderón Villalobos, L.I.A., **Lee, S.**, **De Oliveira, C.**, **Ivetac, A.**, **Brandt, W.**, **Armitage, L. *et al.*** (2012) A combinatorial TIR1/AFB–aux/IAA co-receptor system for differential sensing of auxin. *Nature Chemical Biology*, **8**, 477–485.

Case, D.A. (2018) *Amber 18*. California, San Fr: Univ.

Darden, T., **York, D.** & **Pedersen, L.** (1993) Particle mesh Ewald: an N ·log(N) method for Ewald sums in large systems. *The Journal of Chemical Physics*, **98**, 10089–10092.

Delbarre, A., **Muller, P.**, **Imhoff, V.** & **Guern, J.** (1996) Comparison of mechanisms controlling uptake and accumulation of 2,4-dichlorophenoxy acetic acid, naphthalene-1-acetic acid, and indole-3-acetic acid in suspension-cultured tobacco cells. *Planta*, **198**, 532–541.

dos Santos Maraschin, F., **Memelink, J.** & **Offringa, R.** (2009) Auxin-induced, SCF^{TIR1}-mediated poly-ubiquitination marks AUX/IAA proteins for degradation. *The Plant Journal*, **59**, 100–109.

Eyer, L., **Vain, T.**, **Pařízková, B.**, **Oklestkova, J.**, **Barbez, E.**, **Kozubíková, H. *et al.*** (2016) 2,4-D and IAA amino acid conjugates show distinct metabolism in Arabidopsis. *PLoS One*, **11**, e0159269.

Fehér, A. (2015) Somatic embryogenesis - stress-induced remodeling of plant cell fate. *Biochimica et Biophysica Acta (BBA)-Gene Regulatory Mechanisms*, **1849**, 385–402.

Ferro, N., **Bredow, T.**, **Jacobsen, H.J.** & **Reinard, T.** (2010) Route to novel auxin: auxin chemical space toward biological correlation carriers. *Chemical Reviews*, **110**, 4690–4708.

Ferro, N., **Bultinck, P.**, **Gallegos, A.**, **Jacobsen, H.J.**, **Carbo-Dorca, R.** & **Reinard, T.** (2007) Unrevealed structural requirements for auxin-like molecules by theoretical and experimental evidences. *Phytochemistry*, **68**, 237–250.

Fryer, M.J., **Oxborough, K.**, **Mullineaux, P.M.** & **Baker, N.R.** (2002) Imaging of photo-oxidative stress responses in leaves. *Journal of Experimental Botany*, **53**, 1249–1254.

Gaj, M.D. (2001) Direct somatic embryogenesis as a rapid and efficient system for in vitro regeneration of *Arabidopsis thaliana*. *Plant Cell, Tissue and Organ Culture*, **64**, 39–46.

Garcia, C., **Furtado de Almeida, A.A.**, **Costa, M.**, **Britto, D.**, **Valle, R.**, **Royaert, S. *et al.*** (2019) Abnormalities in somatic embryogenesis caused by 2,4-D: an overview. *Plant Cell, Tissue and Organ Culture*, **137**, 193–212.

Geiss, G., **Gutierrez, L.** & **Bellini, C.** (2009) Adventitious root formation: New insights and perspectives. In: *Root Development*. Oxford, UK: Wiley-Blackwell, pp. 127–156.

Gliwicka, M., **Nowak, K.**, **Balazadeh, S.**, **Mueller-Roeber, B.** & **Gaj, M.D.** (2013) Extensive modulation of the transcription factor transcriptome during somatic embryogenesis in *Arabidopsis thaliana*. *PLoS One*, **8**, e69261.

Guan, Y., **Li, S.G.**, **Fan, X.F.** & **Su, Z.H.** (2016) Application of somatic embryogenesis in woody plants. *Frontiers in Plant Science*, **7**, 938.

Hao, G.F. & **Yang, G.F.** (2010) The role of Phe82 and Phe351 in auxin-induced substrate perception by TIR1 ubiquitin ligase: a novel insight from molecular dynamics simulations. *PLoS One*, **5**, e10742.

Hayashi, K.I., **Neve, J.**, **Hirose, M.**, **Kuboki, A.**, **Shimada, Y.**, **Kepinski, S. *et al.*** (2012) Rational design of an auxin antagonist of the SCF^{TIR1} auxin receptor complex. *ACS Chemical Biology*, **7**, 590–598.

Hayashi, K.-I., **Tan, X.**, **Zheng, N.**, **Hatate, T.**, **Kimura, Y.**, **Kepinski, S. *et al.*** (2008) Small-molecule agonists and antagonists of F-box protein-substrate interactions in auxin perception and signaling. *Proceedings of the National Academy of Sciences of the United States of America*, **105**, 5632–5637.

Horstman, A., **Bemer, M.** & **Boutilier, K.** (2017) A transcriptional view on somatic embryogenesis. *Regeneration*, **4**, 201–216.

Iglesias, M.J., **Terrile, M.C.**, **Correa-Aragunde, N.**, **Colman, S.L.**, **Izquierdo-Álvarez, A.**, **Fiol, D.F. *et al.*** (2018) Regulation of $SCF^{TIR1/AFBs}$ E3 ligase assembly by S-nitrosylation of Arabidopsis SKP1-like1 impacts on auxin signaling. *Redox Biology*, **18**, 200–210.

Jakalian, A., **Jack, D.B.** & **Bayly, C.I.** (2002) Fast, efficient generation of high-quality atomic charges. AM1-BCC model: II. Parameterization and validation. *Journal of Computational Chemistry*, **23**, 1623–1641.

Jin, F., **Hu, L.**, **Yuan, D.**, **Xu, J.**, **Gao, W.**, **He, L. *et al.*** (2014) Comparative transcriptome analysis between somatic embryos (SEs) and zygotic embryos in cotton: evidence for stress response functions in SE development. *Plant Biotechnology Journal*, **12**, 161–173.

Karami, O. & **Saidi, A.** (2010) The molecular basis for stress-induced acquisition of somatic embryogenesis. *Molecular Biology Reports*, **37**, 2493–2507.

Katekar, G.F. (1979) Auxins: on the nature of the receptor site and molecular requirements for auxin activity. *Phytochemistry*, **18**, 223–233.

Koepfli, J.B., **Thimann, K.V.** & **Went, F.W.** (1938) Phytohormones; structure and physiological activity. *The Journal of Biological Chemistry*, **122**, 736–780.

Kouassi, M.K., **Kahia, J.**, **Kouame, C.N.**, **Tahi, M.G.** & **Koffi, E.K.** (2017) Comparing the effect of plant growth regulators on callus and somatic embryogenesis induction in four elite *Theobroma cacao* L. genotypes. *HortScience*, **52**, 142–145.

Larsen, P.B. (2017) Anti-auxin compounds. U.S. Patent 0073308A1.

Lee, R.D.W. & **Cho, H.T.** (2013) Auxin, the organizer of the hormonal/environmental signals for root hair growth. *Frontiers in Plant Science*, **4**, 448.

Lee, S., **Sundaram, S.**, **Armitage, L.**, **Evans, J.P.**, **Hawkes, T.**, **Kepinski, S. *et al.*** (2014) Defining binding efficiency and specificity of auxins for $SCF^{TIR1/AFB}$-aux/IAA Co-receptor complex formation. *ACS Chemical Biology*, **9**, 673–682.

Leyser, O. (2018) Auxin signaling. *Plant Physiology*, **176**, 465–479.

Liao, C.Y., **Smet, W.**, **Brunoud, G.**, **Yoshida, S.**, **Vernoux, T.** & **Weijers, D.** (2015) Reporters for sensitive and quantitative measurement of auxin response. *Nature Methods*, **12**, 207–210.

Livak, K.J. & **Schmittgen, T.D.** (2001) Analysis of relative gene expression data using real-time quantitative PCR and the 2(-Delta Delta C(T)) method. *Methods*, **25**, 402–408.

Ma, Q., **Grones, P.** & **Robert, S.** (2018) Auxin signaling: a big question to be addressed by small molecules. *Journal of Experimental Botany*, **69**, 313–328.

Maier, J.A., **Martinez, C.**, **Kasavajhala, K.**, **Wickstrom, L.**, **Hauser, K.E.** & **Simmerling, C.** (2015) ff14SB: improving the accuracy of protein side chain and backbone parameters from ff99SB. *Journal of Chemical Theory and Computation*, **11**, 3696–3713.

Mantiri, F.R., **Kurdyukov, S.**, **Lohar, D.P.**, **Sharopova, N.**, **Saeed, N.A.**, **Wang, X.D. *et al.*** (2008) The transcription factor MtSERF1 of the ERF subfamily identified by transcriptional profiling is required for somatic embryogenesis induced by auxin plus cytokinin in *Medicago truncatula*. *Plant Physiology*, **146**, 1622–1636.

Nic-Can, G.I., **Galaz-Ávalos, R.M.**, **De-la-Peña, C.**, **Alcazar-Magaña, A.**, **Wrobel, K.** & **Loyola-Vargas, V.M.** (2015) Somatic embryogenesis: identified factors that lead to embryogenic repression. A case of species of the same genus. *PLoS One*, **10**, e0126414.

Nowak, K., **Wójcikowska, B.** & **Gaj, M.D.** (2015) *ERF022* impacts the induction of somatic embryogenesis in Arabidopsis through the ethylene-related pathway. *Planta*, **241**, 967–985.

Peterson, M.A., **McMaster, S.A.**, **Riechers, D.E.**, **Skelton, J.** & **Stahlman, P.W.** (2016) 2,4-D past, present, and future: a review. *Weed Technology*, **30**, 303–345.

© 2023 The Authors.

1365313x, 2023, 5, Downloaded from https://onlinelibrary.wiley.com/doi/10.1111/tpj.16430 by University Of Leiden, Wiley Online Library on [28/11/2023]. See the Terms and Conditions (https://onlinelibrary.wiley.com/terms-and-conditions) on Wiley Online Library for rules of use; OA articles are governed by the applicable Creative Commons License

Prigge, M.J., **Platre, M.**, **Kadakia, N.** ***et al.*** (2020) Genetic analysis of the Arabidopsis TIR1/AFB auxin receptors reveals both overlapping and specialized functions J. Kleine-Vehn, C. S. Hardtke, and J. Kleine-Vehn, eds. *Elife*, **9**, e54740.

Quareshy, M., **Prusinska, J.**, **Kieffer, M.**, **Fukui, K.**, **Pardal, A.J.**, **Lehmann, S.** ***et al.*** (2018) The Tetrazole analogue of the auxin Indole-3-acetic acid binds preferentially to TIR1 and not AFB5. *ACS Chemical Biology*, **13**, 2585–2594.

Rahman, A., **Bannigan, A.**, **Sulaman, W.**, **Pechter, P.**, **Blancaflor, E.B.** & **Baskin, T.I.** (2007) Auxin, Actin and growth of the *Arabidopsis thaliana* primary root. *The Plant Journal*, **50**, 514–528.

Salvo, S.A.G.D., **Hirsch, C.N.**, **Buell, C.R.**, **Kaeppler, S.M.** & **Kaeppler, H.F.** (2014) Whole transcriptome profiling of maize during early somatic embryogenesis reveals altered expression of stress factors and embryogenesis-related genes. *PLoS One*, **9**, e111407.

Shimizu-Mitao, Y. & **Kakimoto, T.** (2014) Auxin sensitivities of all Arabidopsis Aux/IAAs for degradation in the presence of every TIR1/AFB. *Plant & Cell Physiology*, **55**, 1450–1459.

Simon, S., **Kubeš, M.**, **Baster, P.**, **Robert, S.**, **Dobrev, P.I.**, **Friml, J.** ***et al.*** (2013) Defining the selectivity of processes along the auxin response chain: a study using auxin analogues. *The New Phytologist*, **200**, 1034–1048.

Skůpa, P., **Opatrný, Z.** & **Petrášek, J.** (2014) Auxin biology: Applications and the mechanisms behind. In: Nick, P. & Opatrny, Z. (Eds.) *Applied plant cell biology: Cellular tools and approaches for plant biotechnology*. Berlin, Heidelberg: Springer Berlin Heidelberg, pp. 69–102.

Song, Y. (2014) Insight into the mode of action of 2,4-dichlorophenoxyacetic acid (2,4-D) as an herbicide. *Journal of Integrative Plant Biology*, **56**, 106–113.

Tan, X., **Calderon-Villalobos, L.I.A.**, **Sharon, M.**, **Zheng, C.**, **Robinson, C.V.**, **Estelle, M.** ***et al.*** (2007) Mechanism of auxin perception by the TIR1 ubiquitin ligase. *Nature*, **446**, 640–645.

Torii, K.U., **Hagihara, S.**, **Uchida, N.** & **Takahashi, K.** (2018) Harnessing synthetic chemistry to probe and hijack auxin signaling. *The New Phytologist*, **220**, 417–424.

Ulmasov, T., **Murfett, J.**, **Hagen, G.** & **Guilfoyle, T.J.** (1997) Aux/IAA proteins repress expression of reporter genes containing natural and highly active synthetic auxin response elements. *Plant Cell*, **9**, 1963–1971.

Walsh, T.A., **Neal, R.**, **Merlo, A.O.**, **Honma, M.**, **Hicks, G.R.**, **Wolff, K.** ***et al.*** (2006) Mutations in an auxin receptor homolog AFB5 and in SGT1b confer resistance to synthetic Picolinate auxins and not to 2,4-Dichlorophenoxyacetic acid or Indole-3-acetic acid in Arabidopsis. *Plant Physiology*, **142**, 542–552.

Wang, J., **Wolf, R.M.**, **Caldwell, J.W.**, **Kollman, P.A.** & **Case, D.A.** (2004) Development and testing of a general amber force field. *Journal of Computational Chemistry*, **25**, 1157–1174.

Wang, J. & **Yao, L.** (2019) Dissecting C−H···π and N−H···π interactions in two proteins using a combined experimental and computational approach. *Scientific Reports*, **9**, 20149.

Winkler, M., **Niemeyer, M.**, **Hellmuth, A.**, **Janitza, P.**, **Christ, G.**, **Samodelov, S.L.** ***et al.*** (2017) Variation in auxin sensing guides AUX/IAA transcriptional repressor ubiquitylation and destruction. *Nature Communications*, **8**, 15706.

© 2023 The Authors.
The Plant Journal published by Society for Experimental Biology and John Wiley & Sons Ltd.,

1365313x, 2023, 5, Downloaded from https://onlinelibrary.wiley.com/doi/10.1111/tpj.16430 by University Of Leiden, Wiley Online Library on [28/11/2023]. See the Terms and Conditions (https://onlinelibrary.wiley.com/terms-and-conditions) on Wiley Online Library for rules of use; OA articles are governed by the applicable Creative Commons License